molecular pharmaceutics

Article

pubs.acs.org/molecularpharmaceutics

β-Lapachone and Paclitaxel Combination Micelles with Improved Drug Encapsulation and Therapeutic Synergy as Novel Nanotherapeutics for NQO1-Targeted Cancer Therapy

Ling Zhang,[†] Zhen Chen,[†] Kuan Yang,[†] Chun Liu,[†] Jinming Gao,[‡] and Feng Qian*[,†]

[†]Department of Pharmacology and Pharmaceutical Sciences and Collaborative Innovation Center for Diagnosis and Treatment of Infectious Diseases, School of Medicine, Tsinghua University, Beijing 100084, P.R. China

[‡]Simmons Comprehensive Cancer Center, University of Texas Southwestern Medical Center at Dallas, Dallas, Texas 75390, United States

Supporting Information

ABSTRACT: β-Lapachone (LPC) is a novel cytotoxic agent that is bioactivated by NADP(H): quinone oxidoreductase 1 (NQO1), an enzyme elevated in a variety of tumors, such as non-small cell lung cancer (NSCLC), pancreatic cancer, liver cancer, and breast cancer. Despite its unique mechanism of action, its clinical evaluation has been largely hindered by low water solubility, short blood half-life, and narrow therapeutic window. Although encapsulation into poly(ethylene glycol)-*b*-poly(D,L-lactic acid) (PEG−PLA) micelles could modestly improve its solubility and prolong its half-life, the extremely fast intrinsic crystallization tendency of LPC prevents drug loading higher than ∼2 wt %. The physical stability of the LPC-loaded micelles is also far from satisfactory for further development. In this study, we demonstrate that paclitaxel (PTX), a front-line drug for many cancers, can provide two functions when coencapsulated together with LPC in the PEG−PLA micelles; first, as a strong crystallization inhibitor for LPC, thus to significantly increase the LPC encapsulation efficiency in the micelle from 11.7 ± 2.4% to 100.7 ± 2.2%. The total drug loading efficiency of both PTX and LPC in the combination polymeric micelle reached 100.3 ± 3.0%, and the drug loading density reached 33.2 ± 1.0%. Second, the combination of LPC/PTX demonstrates strong synergistic cytotoxicity effect against the NQO1 overexpressing cancer cells, including A549 NSCLC cells, and several pancreatic cancer cells (combination index <1). *In vitro* drug release study showed that LPC was released faster than PTX either in phosphate-buffered saline (PH = 7.4) or in 1 M sodium salicylate, which agrees with the desired dosing sequence of the two drugs to exert synergistic pharmacologic effect at different cell checkpoints. The PEG−PLA micelles coloaded with LPC and PTX offer a novel nanotherapeutic, with high drug loading, sufficient physical stability, and biological synergy to increase drug delivery efficiency and optimize the therapeutic window for NOQ1-targeted therapy of cancer.

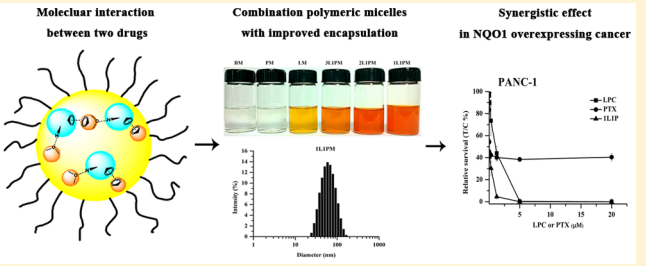

KEYWORDS: *β-lapachone, physical interaction, crystallization, polymeric micelles, therapeutic synergy, NSCLC, pancreatic cancer*

1. INTRODUCTION

β-Lapachone (LPC, Figure 1A) is a novel, plant-derived anticancer agent that was first isolated from the bark of Lapacho tree (genus *Tabebuia*) in the rainforests of South America.[1] It has a long history as an herbal medicine and demonstrates significant antimalarial, antitrypansomal, antibacterial, antifungal, anti-inflammatory, and antineoplastic effects.[2,3] The major cytotoxicity mechanism of LPC against cancer is through NADP(H) quinone oxidoreductase 1 (NQO1) activation.[4] NQO1 is an enzyme that catalyzes two-electron reduction of quinones to protect cells against quinone toxicity.[5,6] LPC can be bioactivated by NQO1 and produce more than ∼120 mol equivalent of H_2O_2 that leads to direct DNA damage, poly(ADP-ribose) polymerase-1 (PARP1) hyperactivation, and ATP loss to induce cell death as "programmed necrosis".[7−9] The anticancer effect of LPC is independent of p53, caspase, cell cycle status,[10,11] which minimizes drug resistance. LPC kills various cancer cells such as non-small cell lung cancer (NSCLC), pancreatic, breast, and liver cancer cells that usually overexpress NQO1.[8,12] For instance, 70% NSCLC and 90% pancreatic cancer demonstrate 10−40-folds of NQO1 overexpression;[9,13,14] therefore, it is highly desirable to evaluate LPC as a potential targeted anticancer agent for these cancers.

Despite its unique mechanism of action, LPC is a poorly soluble compound with aqueous solubility of 0.038 mg/mL.[15] Meanhwile, its blood $t_{1/2}$ is only 24 min and therapeutic window is narrow due to the methemoglobinemia side effect.[16] Although complexation with hydroxylpropyl β-cyclodextrin

Received: June 6, 2015
Revised: August 21, 2015
Accepted: September 28, 2015

DOI: 10.1021/acs.molpharmaceut.5b00448
Mol. Pharmaceutics XXXX, XXX, XXX−XXX

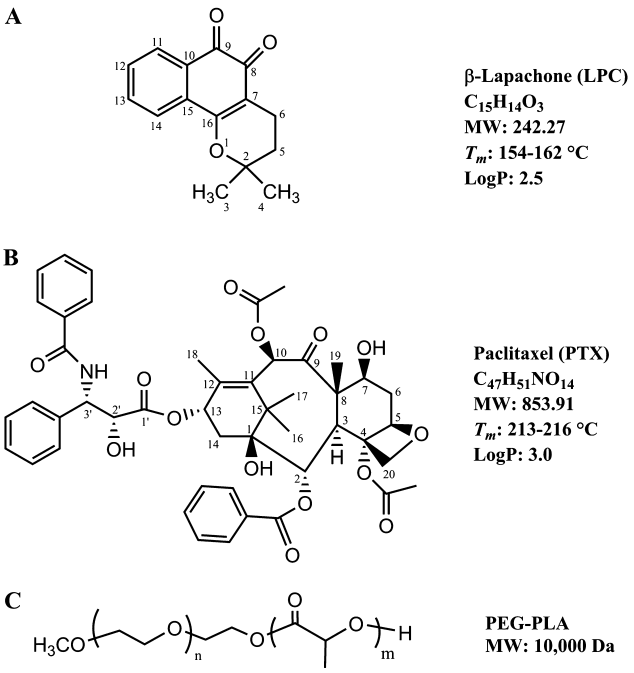

Figure 1. Chemical structures of (A) β-lapachone (LPC), (B) paclitaxel (PTX), and (C) PEG−PLA copolymer.

(HPβ-CD) significantly improved the solubility of LPC,[15] clinical trials were unsuccessful in various cancers,[17−19] largely due to hemolytic anemia, methemoglobinemia, and nonspecific distribution.[16] On the basis of the physicochemical properties of LPC, including low water solubility, fast crystallization rate, low LogP (2.5), and high projected human dose,[18−20] there are limited formulation options to administrate LPC. For instance, LPC is not sufficiently soluble in commonly used pharmaceutical vehicles acceptable for intravenous (IV) administration. The drug does not bind to albumin either, therefore, nab-paclitaxel/Abraxane-like technology is not applicable. Polymeric micelles of diblock copolymers such as poly(ethylene glycol)-*b*-poly(D,L-lactic acid) (PEG−PLA, Figure 1C) represent a nanoscopic drug delivery system that are biocompatible and biodegradable.[21] Paclitaxel PEG−PLA micelles (Genexol-PM) have been approved in South Korea and in phase III study in the United States.[22] Other types of polymeric micelles have also been under clinical evaluations at different stages.[23] The particle size and hydrophilic external PEG layer of PEG−PLA micelles (~5−100 nm) could help them to escape the rapid uptake by the monocular phagocyte system (MPS), and to increase their tumor accumulation through enhanced permeability and retention (EPR) effect.[24,25] Drug loaded polymeric micelles could also be advantageous in prolonging the pharmacokinetic half-life and reducing the C_{max}-induced side effects, which is highly desirable for LPC with short $t_{1/2}$ and related methemoglobinemia side effect.[16] Considering all of the above, LPC encapsulated PEG−PLA micelles have been developed and evaluated *in vitro* and *in vivo*, which showed promising therapeutic strategy against NQO1-overexpressing tumor cells and NSCLC xenografts in mice.[16,26]

Nevertheless, the extremely fast intrinsic crystallization tendency of LPC hampers a PEG−PLA micelle formulation for clinical evaluation and pharmaceutical manufacturing. As reported earlier,[26] the LPC encapsulation efficacy was 41.9 ± 5.6%, and the highest formulation concentration is much lower than 1 mg/mL. Meanwhile, fast crystallization of LPC led to quick precipitation from the PEG−PLA micelles within 1 h (unpublished observation). To improve the encapsulation efficiency of LPC within PEG−PLA micelles, and also to broaden its therapeutic window, we envisioned a combination micelles that coencapsulate both LPC and Paclitaxel (PTX) (Figure 1B), a natural diterpene taxane compound that was originally extracted from *Taxus brevifolia*[27] and currently serves as one of a first line chemotherapy agents against NSCLC, in combination with carboplatin or cisplatin.[28,29] PTX shows a wide spectrum of anticancer activity through stabilization of microtubules to induce G_2/M arrest in tumor cells, which leads to apoptosis,[30] and was developed into a variety of clinical formulations including Taxol (a Cremophor EL-based solvent system), Abraxane (an albumin-bound nanoparticle), Xyotax (a poly(L-glutamic acid)-based PTX conjugate),[21] and Genexol-PM, (a PEG−PLA micelle system[22]) due to its very low aqueous solubility (~0.7 μg/mL) and high hydrophobicity.[21]

The rationales behind LPC/PTX combination PEG−PLA micelles are two-fold. First, potential physical interaction (H-bonding and π−π interaction) might inhibit LPC crystallization and increase drug loading efficiency due to the unique chemical structures of both LPC and PTX. Second, LPC and PTX have a synergistic effect against many cancer cells *in vitro* as well as *in vivo* by the regiment of LPC followed by PTX, or LPC and PTX simultaneously.[31] For example, Antonella D'anneo et al. have studied that the combination of LPC and PTX can synergistically induce apoptosis in human retinoblastoma cells.[30] In this study, we hypothesize that LPC/PTX combination micelles could offer increased drug loading efficiency, formulation stability, and therapeutic synergy for NQO1-targeted therapy of cancer.

2. MATERIALS AND METHODS

2.1. Materials. LPC was synthesized as previously described.[32] PTX was obtained from Ouhe Chemical Co., Ltd. (Beijing, China). Poly(D,L-lactic acid) (PLA5k) (MW = 5000 Da) and PEG5k-PLA5k block copolymer (MW = 10 000 Da) were purchased from Daigang Biotechnology Co., Ltd. (Jinan, China). All organic solvents are of analytical grade. A549 non-small cell lung cancer (NSCLC) cells, PANC-1, and MIA PaCa-2 pancreatic cancer cells were grown in DMEM with 10% fetal bovine serum (FBS). Capan-1 and BXPC-3 pancreatic cancer cells were grown in IMDM with 20% FBS and RPMI-1640 with 10% FBS, respectively. All the culture medium was supplemented with 100 units/mL penicillin, and 100 mg/mL streptomycin. All cells were cultured at 37 °C in a humidified incubator with a 5% CO_2/95% air atmosphere without mycoplasma infection.

2.2. Physical Interaction between LPC and PTX. *2.2.1. Differential Scanning Calorimetry (DSC) Study.* Rapid solvent evaporation was used to prepare LPC/PTX and LPC/PLA mixtures of different compositions. Briefly, 0.1 g of LPC/PTX or LPC/PLA mixtures of 90 wt %, 70 wt %, 50 wt % LPC was dissolved in 2 mL of dichloromethane first, and then the solvent was rapidly evaporated. The obtained solid mixtures were further vacuum-dried at room temperature overnight. The dried LPC/PTX or LPC/PLA samples (4−7 mg) were packed into hermetic aluminum pans with pin holes on the lids and were analyzed by DSC (DSC Q2000, TA Instruments, New Castle, DE, USA). The samples were first heated above the melting point of LPC and then equilibrated at 0 °C for 5 min to allow LPC crystallization. PTX remained amorphous during this time. The samples were then heated up again at a rate of 1

DOI: 10.1021/acs.molpharmaceut.5b00448
Mol. Pharmaceutics XXXX, XXX, XXX−XXX

°C/min until they were completely melted. The melting end-set of the melting events was recorded as T_{end}.[33]

2.2.2. One-Dimensional ^{1}H NMR and ^{13}C NMR. NMR samples were prepared by dissolving LPC, PTX, and their mixtures at molar ratio of 3:1 (3L1P), 2:1 (2L1P), and 1:1 (1L1P) in deuterated chloroform ($CDCl_3$). LPC concentration in all solutions was 40 mg/mL. The samples were then analyzed by a 400 MHz NMR spectrometer (^{1}H NMR, Bruker Biospin GmbH, Rheinstetten, Germany) or a 100 MHz NMR spectrometer (^{13}C NMR, Bruker Biospin GmbH, Rheinstetten, Germany) at 25 °C.

2.2.3. Fourier Transform Infrared (FT-IR) Study. The FT-IR samples were prepared by rapid solvent evaporation. The dried samples were analyzed by a Fourier transform infrared spectrometer (Bruker Optics, Vextex 70, Ettlingen, Germany) to evaluate potential H-bonding interactions. FT-IR spectra were scanned from 400−4000 cm^{-1} with a resolution of 4 cm^{-1}.

2.3. Supersaturation Kinetics of LPC in Aqueous Solution with and without the Presence of PTX. The supersaturation kinetics of LPC with or without the coexistence of PTX was compared. Briefly, pure LPC or the LPC/PTX mixture at 3:1 molar ratio (3L1P) was dissolved in methanol to make a solution at 5 mg/mL LPC concentration. The solutions were then diluted 10 times with PBS (PH = 7.4) to generate ~14-times the LPC supersaturation (solubility of LPC: 38 μg/mL) and then placed on a shaker at 37 °C. After 2, 5, 10, 15, 20, and 25 min, samples were withdrawn and filtered through 0.45 μm membrane filters. The solution LPC concentration in the supernatant was measured by high-performance liquid chromatography (HPLC). All experiments were performed in triplicate. The precipitated drugs were vacuum-dried and then observed by scanning electron microscope (SEM, FEI Quanta 200 Czech).

2.4. Fabrication and Characterization of LPC-, PTX-, and LPC/PTX-Loaded PEG−PLA Micelles. *2.4.1. Drug Encapsulation Efficiency and Density.* Polymer micelles loaded with LPC, PTX, or a combination of LPC and PTX were prepared by a film hydration method. Briefly, PEG−PLA and appropriate amount of drug(s) were dissolved in acetonitrile. The solvent was evaporated by a rotary evaporator at 60 °C to form a thin film. Normal saline at 60 °C was then added to hydrate the film under sonication for 5 min. The resulted aqueous solution of drug-loaded polymer micelles was filtered through 0.45 μm membrane filters to remove aggregates of nonencapsulated drugs. The obtained micelle formulations were summarized in Table 1.

The drug loading efficiency, drug loading density, and yield of micelle formulations were determined and calculated according to previously reported methods:[26]

$$\text{Encapsulated drug loading efficiency} = \frac{\text{encapsulated drug in micelles}}{\text{amount of drug used to prepare micelles}} \times 100$$

$$\text{Encapsulated drugs loading density} = \frac{\text{encapsulated drug in micelles}}{\text{weight of the dried micelles}} \times 100$$

where the amount of encapsulated-drug in the micelles was calculated by the total amount of drug in the micelle solution, minus the amount of free drug (drug solubility times solution volume).

Table 1. PEG−PLA Micelle Formulations Encapsulated with PTX, LPC, or LPC/PTX Combinations

micelle system	LPC/PTX molar ratio[a]	theoretical LPC weight percentage (wt %)[a]	theoretical total drugs weight percentage (wt %)	abbreviation
black micelle	N/A	N/A	N/A	BM
PTX micelle	N/A	N/A	10	PM
LPC micelle	N/A	10	10	LM
3:1 LPC/PTX micelle	3:1	9.1	18	3L1PM
2:1 LPC/PTX micelle	2:1	8.3	25	2L1PM
1:1 LPC/PTX micelle	1:1	7.7	31	1L1PM

[a]N/A, not applicable.

2.4.2. Confirmation of the Core−Shell Architecture of the Micelles Using ^{1}H NMR Spectroscopy. Freeze-dried micelle samples (LM, PM, 3L1PM) were dissolved in $CDCl_3$. The 3L1PM was also dissolved in D_2O. ^{1}H NMR spectroscopy (Bruker 400 MHz) was used to confirm the encapsulation of drugs within the PEG−PLA micelles through the comparison of NMR spectra of the samples dissolved in $CDCl_3$ and D_2O.

2.4.3. Particle Size and Morphology of the Micelles. The particle size of the freshly prepared micelles was analyzed at 25 °C by dynamic light scattering (DLS, Malvern Instruments Inc., U.K.) at scattering angle of 90°. The morphology of the polymer micelles was studied by transmission electron microscopy (FEI Tecnai Spirit Bio TWIN TEM D1297, USA) with negative staining of phosphotungstic acid.

2.4.4. In Vitro Drug Release Kinetics from the Micelles. Drug release study was carried out in two different aqueous media with different sink conditions. Briefly, 0.5 mL of the drug encapsulated micelle solution with 0.5 mL normal saline was added into a dialysis tube (MWCO = 100 000 Da, Spectrum Float-A-Lyzer), which was then dialyzed against 80 mL of PBS or 80 mL of 1 M sodium salicylate[34] at 37 °C with slow agitation. At predetermined time points (0.5, 1, 3, 5, 7, and 24 h), 0.5 mL of release medium was removed and replaced with an equal volume of fresh medium. Drug concentration in the withdrawn medium was analyzed by HPLC.

2.4.5. In Vitro Cytotoxicity against NQO1 Overexpressing NSCLC and Pancreatic Cancer Cell Lines. Relative survival of A549 lung cancer cells after exposed to different micelle formulations was studied using Cell Counting Kit-8 (CCK-8) and DNA dye Hoescht 33258. Briefly, A549 cells were first seeded into 96-well culture plates (5000 cells/well) and 96-well opaque plates (3000 cells/well) with 0.1 mL of cell culture medium for CCK-8 and DNA assays, respectively. After cell culture of 24 h, the cell culture medium was removed and replaced with micelle solution in 0.2 mL of cell culture medium. The cells were further incubated for 4 h, and then the drug containing medium was removed, and control growth medium was added. Since A549 NSCLC cells overexpress NQO1, dicoumarol (40 μM), a NQO1 competitive inhibitor, was used to study the NQO1 specific cytotoxicity. The cell metabolic activity was measured by CCK-8 immediately after 4 h exposure to different micelles and washed with 0.2 mL of

DOI: 10.1021/acs.molpharmaceut.5b00448
Mol. Pharmaceutics XXXX, XXX, XXX−XXX

PBS per well, and the results were obtained by a microplate reader (Molcular Devices, SpectraMax Plus 384, US). Cells were allowed to grow for an additional 7 days, and then their DNA content was determined by fluorescence of DNA dye Hoescht 33258 on PerkinElmer EnVision machine (Waltham, MA), adapting a method by Labarca and Paigen.[35] Data were expressed as means ± STD relative growth and graphed as treated/control (T/C) values from six wells per treatment.

Similarly, relative survival of four pancreatic cancer cells after exposed to different drug solutions (DMSO) was studied using CellTiter-Glo (CTG) assay kit (Promega). Briefly, pancreatic cancer cells were seeded to 384-well white plate (600 cells/well, 3 wells/group) with 27 μL of cell culture medium. After 24 h, the cell culture medium was removed and replaced with different drug solutions mixed with cell culture medium. Cells were further incubated for 48 h and then equilibrated at room temperature for 30 min. Thirty microliters of the CellTiter-GloReagent was added to each well in the 384-well plate. After cell lysis, all the plates were allowed to incubate at room temperature for 10 min to stabilize luminescent signal. Data of relative survival were recorded luminescence with EnVision 2104 Multilabel Reader. All data were calculated IC_{50} by using GraphPad Prism 5 software.

Combination index (CI) analyses were performed using CompuSyn software (Version 1.0, CompuSyn Inc., U.S.) based on a method reported by Chou and Talalay.[36] CI and Fa-CI (Fa is the fraction of affected cells) plots for PTX and LPC were calculated according to the User's Guide of CompuSyn 1.0. By this calculation, CI = 1 indicates additive effect in the absence of synergism or antagonism, CI < 1 indicates synergism, while CI > 1 indicates antagonism.

3. RESULTS AND DISCUSSION

3.1. Crystallization Propensity of LPC. As shown by the chemical structure of LPC (Figure 1A), LPC molecules could form intermolecular interaction through the $\pi-\pi$ stacking between their naphthoquinone rings, as well as through a weaker C−H···O hydrogen-bonding,[37] and crystallize very rapidly.

Morphologically, LPC is a needle-like crystal at room temperature with intense and characteristic yellow to orange color (Figure 2A). After melted at 170 °C by a DSC, the molten LPC rerecrystallized extremely fast upon cooling and the recrystallization process completed within 1 min once the temperature decreased below ∼120 °C and formed spherulitic crystal structure (Figure 2B). The recrystallization behavior during cooling can be used as an indicator as the crystallization tendency of the drug. Drugs that completely crystallize at cooling from melt are usually considered as fast crystallizers.[38] Furthermore, the recrystallization of LPC occurred so fast that a conventional DSC could not even respond fast enough to record this exothermic heat exchange event (∼130−120 °C) as a peak but as a narrow loop (Figure 2C). The extremely fast crystallization tendency is the major reason causing physical instability of the LPC in the PEG−PLA micelles.

3.2. Physical Interaction between LPC, PTX, and PLA. Considering the chemical structure of PTX and LPC, we hypothesize that PTX might be able to inhibit the molecular mobility of LPC and thus the crystallization of LPC, due to the possibility of H-bonding formation between the PTX −OH groups and the LPC -C═O groups, as well as the possible $\pi-\pi$ interaction between the benzyl rings of the two different molecules. To confirm the existence of these intermolecular interactions, the physical interaction between LPC and PTX was investigated by thermal analysis, ^{1}H NMR, and FT-IR.

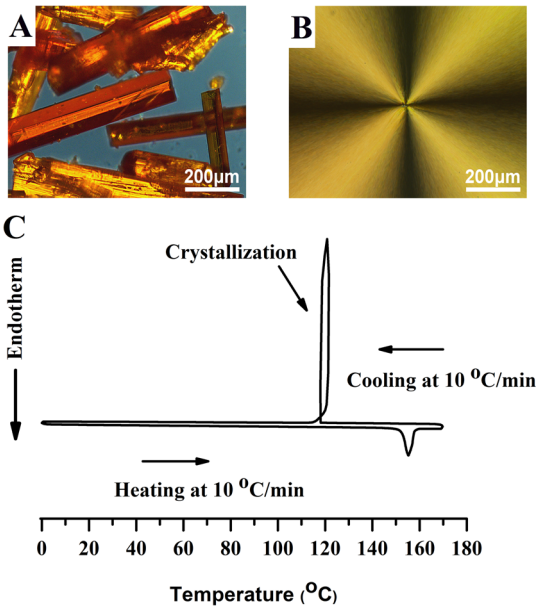

Figure 2. (A) LPC crystals under polarized light microscope. (B) Molten LPC recrystallized within 1 min after cooling below the recrystallization temperature (∼120 °C) at 10 °C/min cooling rate. (C) The DSC curve of the melting and recrystallization of LPC. Because of the extremely fast LPC crystallization rate, the recrystallization event appears to be a narrow loop (heating and cooling rate of DSC: 10 °C/min).

The extent of melting point depression of a crystalline substance in the presence of another amorphous material is an indication of the strength of the intermolecular physical interaction.[39,40] With stronger attractive interaction between two molecules, the mixing between them becomes more favorable (i.e, more negative free energy of mixing); thus, the dissolution of certain amount of crystalline drug (LPC in this case) in another amorphous material (PTX or PLA in this case) could occur at a lower temperature.[38,41] Shown in Figure 3, panel A, the extent of LPC melting depression, that is, the gap between T_{end} of a LPC/PTX mixture and the T_{onset} of LPC, increases with the increase of PTX percentage. More quantitatively, the Flory−Huggins interaction parameter (χ) between LPC and PTX could be calculated using a reported method.[38,41] The calculated χ value between LPC and PTX is −0.01, a negative value that indicates attractive intermolecular interaction. In comparison, we concluded that the hydrophobic PLA core of the PEG−PLA micelles, which directly contact with the encapsulated LPC molecules, does not interact strongly with LPC. This was demonstrated by the less extent of melting depression of LPC by PLA, compared with that by PTX (Figure 3B), as well as a positive Flory−Huggins interaction parameter between LPC and PLA at 0.11, an indication of the absence of attractive interaction between the two. In summary, the above thermal analysis demonstrated that in the solid state, PTX strongly interacts with LPC and thus could inhibit its crystallization. This effect could improve LPC drug encapsulation within the PEG−PLA micelle, whereas the PLA segments within the micelle core are not effective crystallization inhibitors for LPC (as observed earlier[26] and in this work).

DOI: 10.1021/acs.molpharmaceut.5b00448
Mol. Pharmaceutics XXXX, XXX, XXX−XXX

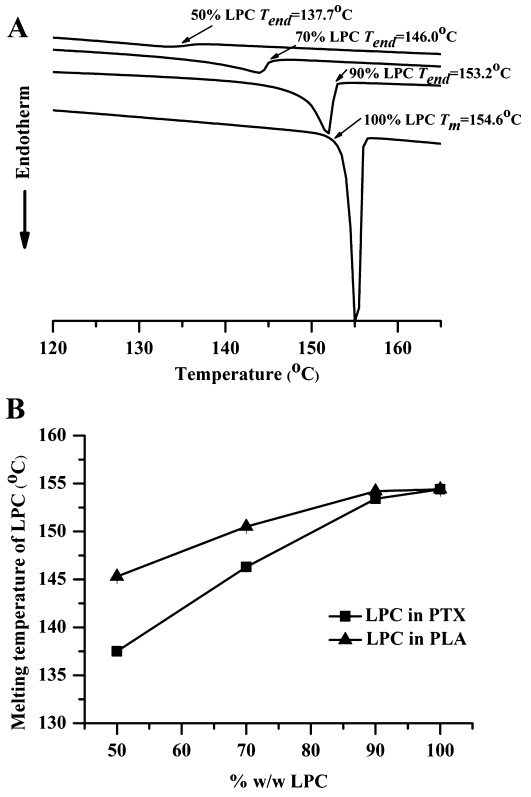

Figure 3. DSC analysis of LPC melting depression in the presence of amorphous PTX or PLA. (A) DSC traces of the melting of LPC crystals in the presence of different weight percentage of amorphous PTX (heating rate: 1 °C/min). (B) Melting of LPC in the presence of PTX or PLA. The melting onset was used as the melting temperature of the pure LPC crystal, and the melting end set was used as the melting temperature of LPC in the presence of PTX or PLA (n = 2, average value reported).

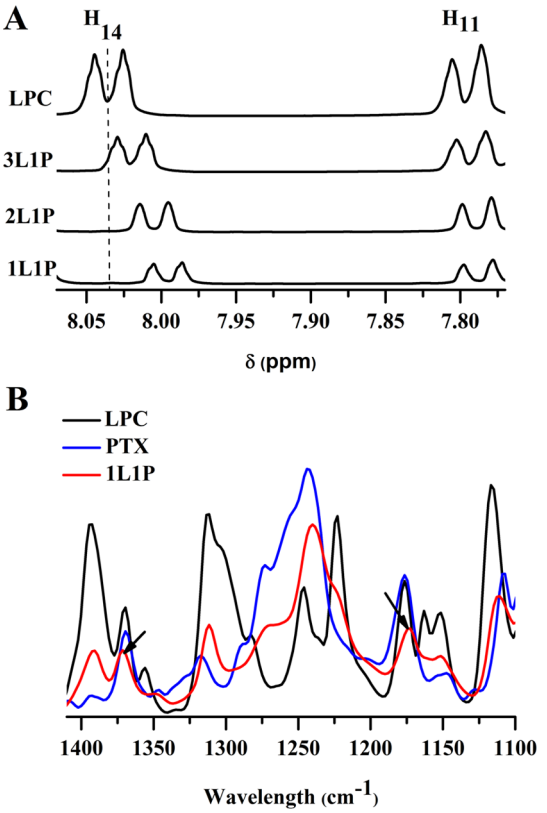

Figure 4. (A) ^{1}H NMR spectra of LPC/PTX at different molar ratios, that is, 3:1 (3L1P), 2:1 (2L1P), and 1:1 (1L1P), in $CDCl_3$. The chemical shift of 7.26 ppm from $CDCl_3$ as reference signal. (B) FT-IR spectra of LPC, PTX, and LPC/PTX solid mixtures (1:1 molar ratio, 1L1P) prepared by solvent evaporation. Arrows indicate shifts of the wavenumbers.

For ^{1}H and ^{13}C NMR analysis, the LPC/PTX interaction was investigated at the molecular level (Figure 4A and Table 2). In Figure 4, panel A, with the addition of PTX into the LPC solution, the LPC H14 chemical shift changed substantially to the upfield, and the extent of shift was proportional to the LPC/PTX molar ratio (i.e., 1L1*P* > 2L1*P* > 3L1*P* > LPC). Also, the addition of PTX significantly shifted C16 to downfield ($\Delta\delta$ = +0.19, listed in Table 2). On the other hand, the existence of LPC significantly influenced the benzene ring, −NH, and −OH groups of PTX. The PTX peaks of C1′, C10 AcO CO, N3′Ph C═O, C3′NPh-i, C3′NPh-p, C3′Ph-m C3′NPh-m, C3′Ph-p, C2Ph-I, C4, C7, C13 shifted to upfield, and C12, C3′Ph-i, C2′, C13 to downfield. This result indicates the formation of H-bonding or $\pi-\pi$ interaction between LPC and PTX, which inhibits the crystallization of LPC.

FT-IR analysis (Figure 4B) showed peak 1369 cm^{-1} shifted to 1371 and 1176 cm^{-1} shifted to 1173 cm^{-1} of LPC. The peak centers 1369 and 1176 cm^{-1} are the group of C−O−C in LPC. The FT-IR result indicated that the C−O−C group interacts with some groups of PTX, which was proved by NMR study.

3.3. PTX Inhibits LPC Crystallization in Aqueous Solution. We observed that PTX not only significantly inhibited LPC crystallization in the dry state, but also in the aqueous environment. As shown in Figure 5, panel A, an oversaturated (~14-times of solubility) amount of LPC was introduced into PBS buffer either as a single drug or together with PTX. The presence of PTX in PBS buffer solution can significantly prolong the supersaturation of LPC, which otherwise can only be maintained for a much shorter period. The existence of PTX clearly hindered the crystallization of LPC, as the precipitated LPC showed: without the presence of PTX, LPC crystallized into large, needled sharp single crystals

Table 2. Change of ^{13}C NMR Chemical Shifts ($\Delta\delta$ ^{13}C) of LPC and PTX in $CDCl_3$ Solution Compared with the Pure Drug Solution at the Same Concentration[a]

	$\Delta\delta$ ^{13}C		$\Delta\delta^{13}$C
carbon number	LPC	carbon number	PTX
C16	0.19	C1′	−0.13
		C10 AcO CO	−0.14
		N3′Ph C═O	−0.21
		C12	0.15
		C3′Ph-i	0.15
		C3′NPh-i	−0.33
		C3′NPh-p	−0.28
		C3′Ph-m C3′NPh-m	−0.28
		C3′Ph-p	−0.26
		C2Ph-i	−0.33
		C4	−0.24
		C2′	0.12
		C7	−0.29
		C13	−0.37
		C3′	0.18

[a]The chemical shift of 77.16 ppm from $CDCl_3$ as reference signal.

DOI: 10.1021/acs.molpharmaceut.5b00448
Mol. Pharmaceutics XXXX, XXX, XXX−XXX

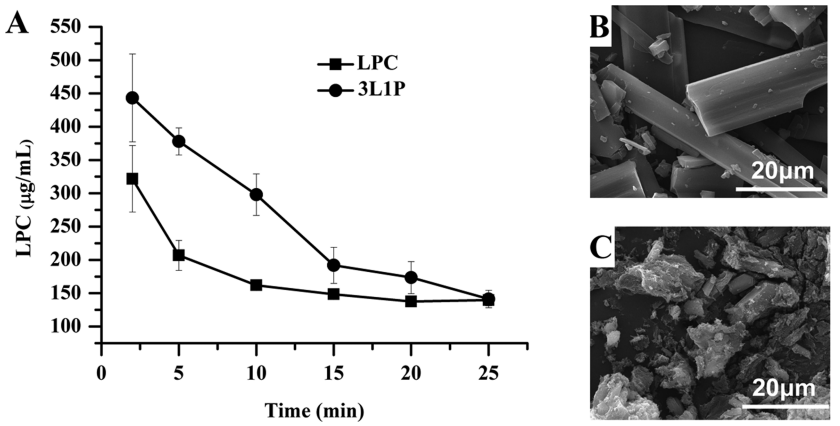

Figure 5. (A) Supersaturation profiles of LPC in the presence (0.5 mg/mL) and absence of PTX in PBS (PH = 7.4) at 37 °C. (B) SEM image of pure LPC. (C) SEM image of the precipitated LPC in the presence of PTX (0.5 mg/mL) in PBS.

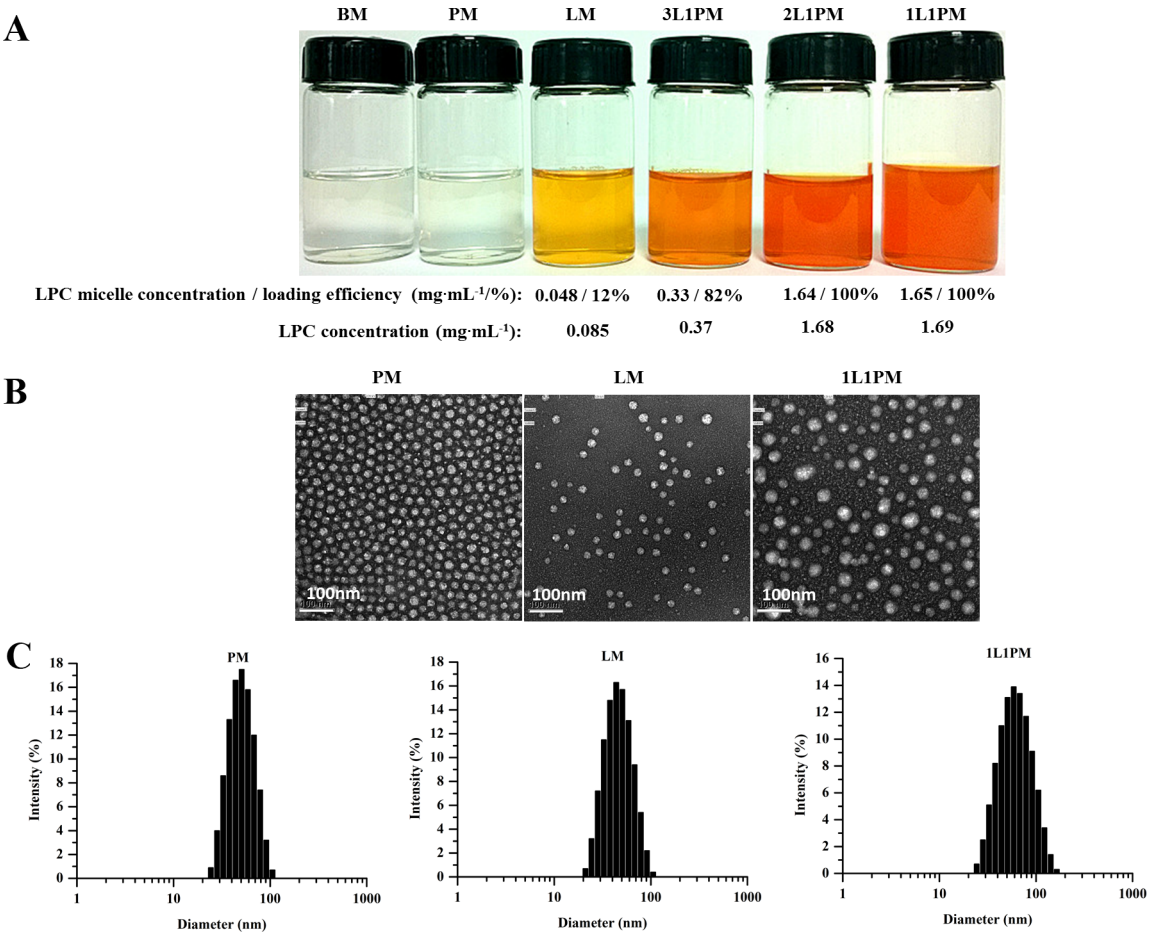

Figure 6. (A) Visual appearance of the micelle solutions. (B) TEM images of the micelles. (C) Particle size distribution of different micelles measured by dynamic light scattering (DLS).

with >10 μm in width and tens of μm in length (Figure 5B), while with the presence of PTX, no large size LPC single crystals with perfect needle sharp morphology could be observed (Figure 5C). The results clearly showed that the crystallization of LPC was significantly disrupted by PTX.

It is worth noting that in the research area of amorphous drug−polymer solid dispersion for oral bioavailability enhancement of poorly water-soluble drugs, it is well-known that drug supersaturation could be prolonged in aqueous solution by various water-soluble polymers, such as hydroxypropyl methylcellulose acetate succinate (HPMC-AS), polyvinylpyrrolidone vinyl acetate (PVP-VA), polyvinylpyrrolidone (PVP), etc., which form H-bonding, dipole−dipole interaction, or other intermolecular interactions with the drugs.[42] However, these polymers are not used in FDA approved intravenous injection products at any substantial level. In the current study, PTX serves a similar role as these polymers to physically inhibit LPC crystallization and to improve drug encapsulation, yet PTX has its second role as a pharmacologically active anticancer agent,

DOI: 10.1021/acs.molpharmaceut.5b00448
Mol. Pharmaceutics XXXX, XXX, XXX−XXX

which acts synergistically with LPC against NQO1 overexpressing cancer cells, as discussed later.

3.4. Physical Characterization of Various Drug Encapsulated PEG−PLA Micelles. We prepared various PEG−PLA micelles loaded with PTX, LPC, and different ratios of LPC/PTX to confirm the effect of PTX to improve the LPC encapsulation efficiency.

The visual appearance, TEM morphology, and particle size distribution of different drug encapsulated micelles are shown in Figure 6A−C, respectively. The pure PTX micelle (PM, Figure 6A) is colorless, while pure LPC micelle (LM, Figure 6A) with ∼0.085 mg/mL concentration is orange. The LPC encapsulation within the PEG−PLA micelles improved significantly with the increase of LPC/PTX ratio, as shown clearly by the increased color intensity of the LPC/PTX coencapsulated micelles. On the basis of the visual comparison, a LPC/PTX molar ratio about 3:1 (3L1P) could substantially increase LPC encapsulation efficiency and increase the concentration of micelle solution (Figure 6A). Inspected by TEM, all drug-loaded micelles appear to be spherical nanoparticles with particle sizes range from 40−70 nm (Figure 6B). Their particle size distribution was analyzed by dynamic light scattering and compared in Figure 6, panel C. The particle size distribution of LPC/PTX coencapsulated micelles appeared to less uniform in particle size compared with the pure LPC and PTX micelles, although they remained monodisperse and are within a small size range (mostly under 50 nm). The size of these nanoparticles fell into the reported optimal size range of nanomedicine[43] for solid tumor drug delivery, presumably by the EPR effect.[44]

To confirm the core−shell structure of the micelles with drug encapsulated within the hydrophobic inner core, LPC encapsulated and PTX encapsulated micelles were dissolved in $CDCl_3$, while LPC/PTX coencapsulated micelles were dissolved in both $CDCl_3$ and D_2O, and their ^1H NMR spectra were collected and compared (Figure 7), similarly as a previously reported methodology.[26] The ^1H NMR spectra of the $CDCl_3$ micelles solutions showed all the resonance peaks of the encapsulated drugs and PEG−PLA polymer between 6.0 and 8.0 ppm, while the D_2O micelle solution of the LPC/PTX micelle with same concentration showed no drug or polymer peaks within the same chemical shift region, indicating the absence of free polymer or free drugs in the D_2O solution. This ^1H NMR analysis result, together with the TEM pictures, jointly confirmed the core−shell structure of the drug encapsulated micelles with drugs contained in the hydrophobic inner core.

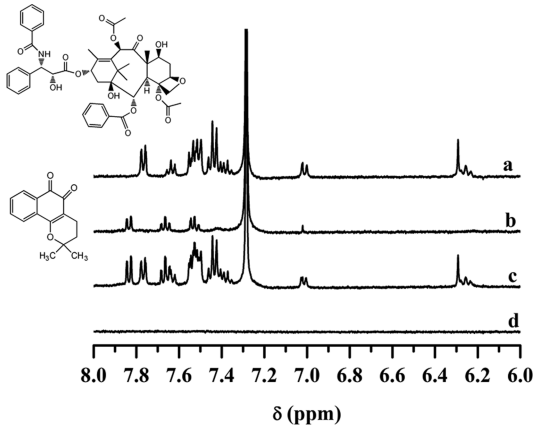

Figure 7. ^1H NMR spectra of the polymeric micelles. (a) PM in $CDCl_3$. (b) LM in $CDCl_3$. (c) 3L1PM in $CDCl_3$. (d) 3L1PM in D_2O. The absence of NMR peaks of either PTX or LPC in panel d indicates that the majority of the drugs were encapsulated within the polymer micelles.

Table 3 listed the key formulation parameters of various micelles. The pure LPC micelle (LM) only has a drug loading density of 1.3% and drug loading efficiency of 11.7%, while the 1:1 LPC/PTX coencapsulated micelle (1L1PM) has a total drug loading density of 33.2% and almost 100% drug loading efficiency for both drugs. This represents a ∼26-fold increase in the total drug loading density, or ∼13-times increase in the LPC loading density in the micelles. We also observed that the particle size distribution and the micelle drug concentration of LPC/PTX coencapsulated micelles (2L1PM, 1L1PM) remained constant within 48 h. Overall, 3L1PM, 2L1PM, and 1L1PM yielded more stable polymer micelles with higher LPC content compared to LM. The much increased LPC loading, as well as the synergistic effect with PTX (discussed later), resolved the formulation difficulty in intravenous delivery of this promising anticancer agent and made any future *in vivo* evaluation and formulation development possible.

3.5. *In Vitro* Drug Release of the Polymeric Micelle Systems. Coencapsulation of different drugs into the micelles could alter the hydrophobicity of the inner core of the nanoparticles and the self-assembly behavior of the micelles. The existence of molecular interaction between the coloaded drugs, as well as that between the drug and the polymer, could also influence the release kinetics of both drugs from the micelles and cause different pharmacokinetic behavior. The release kinetics is critical for the combination micelles to achieve synergistic anticancer effect *in vivo* because the optimal synergy of any drug combination is dose ratio and dosing sequence dependent.[45] To understand the release kinetics of LPC and PTX from different combination micelles, we compared the drug release kinetics from PTX, LPC, and combination (1L1PM and 3L1PM) micelles in PBS (PH = 7.4) and 1 M sodium salicylate, a release medium that provides a better sink condition for hydrotropic drugs.[34]

In PBS (Figure 8A), LPC released similarly from the combination micelles as from the single agent micelles, with a release $t_{1/2}$ (i.e., time that 50% drug release) of ∼5 h. As a hydrophobic drug (LogP ≈ 3.0), PTX did not show detectable release from the PM and 1L1PM within 20 h in PBS. Two factors could have contributed to the much faster LPC release compared with PTX: first, the solubility of LPC is roughly two orders of magnitude higher than that of PTX, which could certainly increase it release rate; second, as a molecule that does not interact with PLA strongly (Figure 2B), there is no sufficient molecular interaction within the drug/PLA hydrophobic core to delay its release. In contrast, with the abundant functional groups and more complex three-dimensional configuration of PTX, there are more opportunities for PTX/PLA molecular interaction. Together with a much lower solubility, the slower PTX release is conceivable.

Interestingly, the PTX release rate was accelerated by the coencapsulation of LPC: about ∼18% of PTX released from the LPC/PTX combination micelles (3L1PM) after 18 h in PBS (Figure 8A) and about 50% of PTX released from the LPC/PTX combination micelles at 3:1 molar ratio (3L1PM) after 3 h the 1 M sodium salicylate solution (Figure 8B, compared with PTX from the pure PTX micelle). Without a definitive

DOI: 10.1021/acs.molpharmaceut.5b00448
Mol. Pharmaceutics XXXX, XXX, XXX−XXX

Table 3. Formulation Comparison between Different PEG−PLA Micelles (n = 3). Stability of the Polymer Micelles Was Monitored by DLS

micelle samples	theoretical total drugs loading density (wt %)	micelle size (nm)	polydispersity	LPC loading efficiency (%)	total drugs loading efficiency (%)	total drugs loading density (wt %)	stability (h) at 25 °C	stability (h) at 4 °C
PM	10	46.4 ± 1.7	0.13 ± 0.03	N/A[a]	102.6 ± 1.0	10.2 ± 0.4	~6	~24
LM	10	40.8 ± 1.8	0.08 ± 0.01	11.7 ± 2.4	11.7 ± 2.4	1.3 ± 0.4	~12	~24
3L1PM	18	49.1 ± 0.6	0.09 ± 0.01	82.1 ± 9.9	95.6 ± 8.4	17.2 ± 0.4	~12	~24
2L1PM	25	58.9 ± 2.2	0.16 ± 0.02	100.1 ± 3.1	100.9 ± 4.2	26.7 ± 0.6	~12	~48
1L1PM	31	63.1 ± 2.4	0.15 ± 0.01	100.7 ± 2.2	100.3 ± 3.0	33.2 ± 1.0	~24	>48

[a]N/A, not applicable.

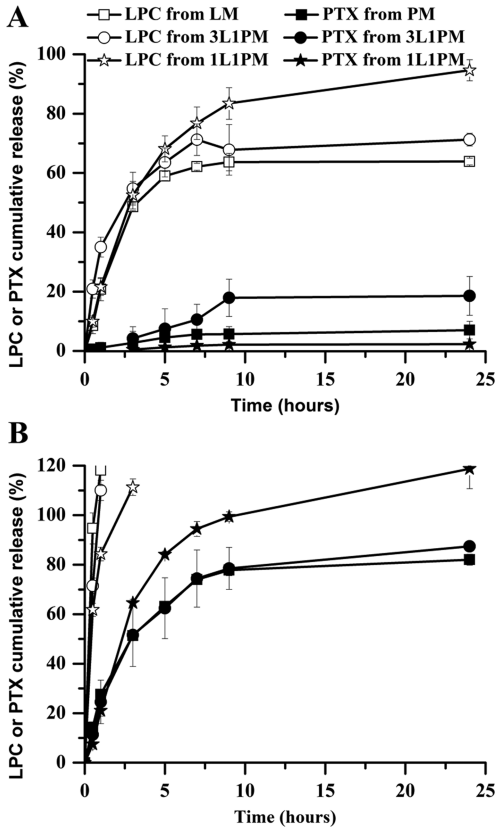

Figure 8. *In vitro* PTX and LPC release kinetics from the micelle formulations. (A) Drug release kinetics in PBS at 37 °C with gentle stirring. (B) Drug release kinetics in 1 M sodium salicylate at 37 °C with gentle stirring.

molecular mechanism, we hypothesize that the existence of LPC might have replaced the stronger PTX−PLA interaction with a weaker PTX−LPC interaction. Also, without a decrease of PTX loading (10%) within the PLA core, coencapsulation of another equal amount of LPC certainly will increase the free energy of the hydrophobic core, thus to increase the PTX release rate. The release $t_{1/2}$ of PTX from either the combination micelles (3L1PM) and single agent micelles (PM) was ~3 h, while 100% LPC released from combination or single agent (LM) micelles within 1 h. In the more stable micelle system (1L1PM), although both of the drugs released slower than them in 3L1PM, LPC still released fast in both of the two different release medium systems (Figure 8). Apparently, regardless of the release conditions, PTX always released slower than LPC from the coencapsulated micelles, presumably due to its much lower solubility and stronger molecular interaction with PLA. This could be pharmacologically beneficial due to the fact that LPC induces delays in the G_1/S phase, and PTX induces G_2/M arrest of cancer cells. The different enhanced effects on cycle checkpoints can recruit more cancer cells into checkpoint-mediated apoptosis.[31] The LPC/PTX combination of two stage release profiles from single nanoparticle could impose tumor killing by dynamic rewiring of signaling pathways to enhance synergistic tumor cytotoxicity effect.[46]

3.6. *In Vitro* Cytotoxicity of LPC/PTX Combination against NQO1 Overexpressing NSCLC and Pancreatic Cancer Cells. First, we studied the time-dependent and dose-dependent cytotoxicity of LPC/PTX combination against A549 cells, a NQO1 overexpressing NSCLC cell line, using the CCK-8 assay to rapidly measure the cell cytotoxicity of different micelles. The cytotoxicity of PTX in PM and 3L1PM was not observed in the assay because of two potential reasons: (1) PTX released slowly from the micelles (Figure 8), and (2) the cytotoxic action of PTX against A549 cells is relatively slow. After a 4-h cell treatment, the LPC micelle (LM) or the LPC/PTX combination micelle (3L1PM) both displayed similar cytotoxicity against the A549 cells (Figure 9A). Figure 9, panel A suggested that LPC released fast from 3L1PM micelles and can quickly produce cytotoxicity against NQO1 overexpressing cancer cells. The result was consistent with our *in vitro* release study. To confirm the NQO1 specific cytotoxicity of LPC/PTX micelle toward the A549 NSCLC cells, we used dicoumarol (40 μM), a NQO1 competitive inhibitor, to inhibit the enzyme function of NQO1. Obviously, the cytotoxicity of LPC micelle (LM) toward A549 cells was significantly decreased when DIC was added (Figure 9). In contrast, since the cytotoxicity of PTX toward A549 is not NQO1 specific, we observed little difference in PTX cytotoxicity toward A549 cells with (PM DIC) or without (PM) the presence of DIC.

To investigate the long-term survival of A549 cells after the 4 h exposure to different micelle formulations, the cells were cultured for an additional 7 days with fresh cell culture medium. After 7 days, the relative cell survival in the PM, 3L1PM, panels appeared to be much lower than the LM panels (Figure 9B). The IC_{50} values of LM, PM, and 3L1PM for A549 cells were 4.5, 0.32, and 0.16 μM, respectively, calculated by GraphPad Prism5 based on the DNA assay data. Because PTX is a much more cytotoxic agent (IC_{50} = 0.32 μM) for the A549 cells compared with LPC (IC_{50} = 4.5 μM), the observed A549 cell survive curve with the application of 3L1PM appears to be relatively close to that of pure PTX micelles (PM). However, the calculated IC_{50} value of the combination micelle (3L1PM) was 0.16 μM, much lower than that of PM. Furthermore, the calculated combination index (CI) value between LPC and PTX in the A549 cytotoxic study was less than 1, indicating cytotoxic synergistic effect between LPC and PTX in the A549 NSCLC cells (Figure 9C).

DOI: 10.1021/acs.molpharmaceut.5b00448
Mol. Pharmaceutics XXXX, XXX, XXX−XXX

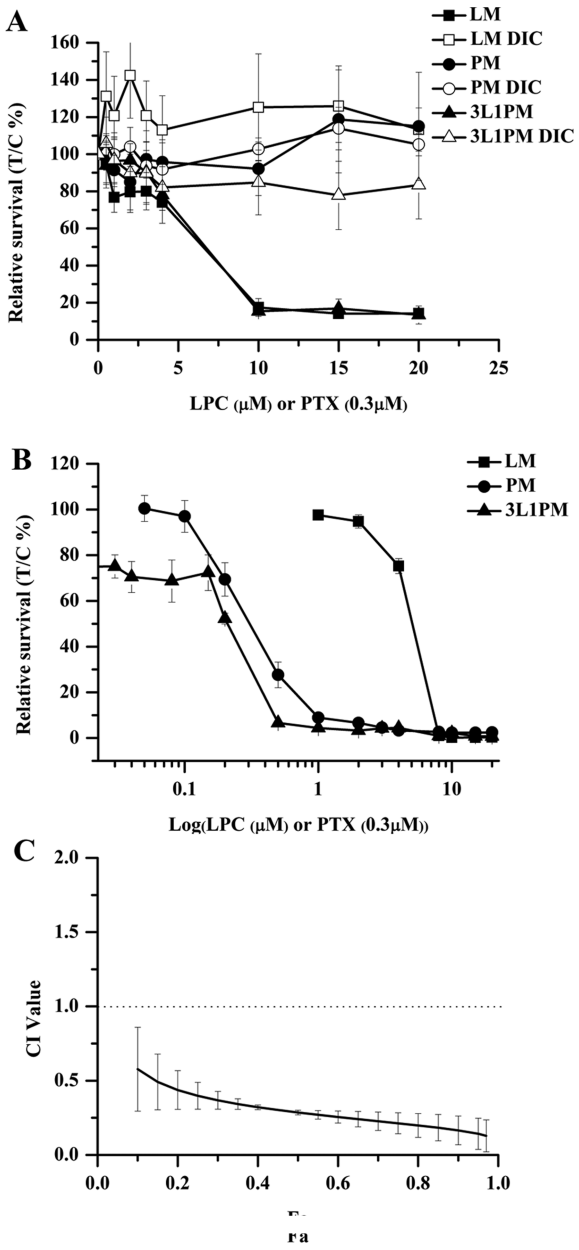

Figure 9. Cytotoxicity of different micelles (LM, PM, 3L1PM) against A549 NSCLC cells at indicated doses. Dicoumarol (DIC, 40 μM) was used as a competitive inhibitor in the studies. (A) Cell viability with CCK-8 assay after 4 h of micelles exposure. (B) Cell viability based on DNA content with Hoescht dye 33258 after the cells were exposed to different micelles for 4 h, followed by growth for an additional 7 days. (C) CI analysis of the combination micelles.

Pancreatic cancer currently is the fourth death causing cancer in United States and is expected to be second in several years, only after lung cancer,[47] due to the many reasons including lack of effective therapeutics.[48,49] Since pancreatic cancer cells also significantly overexpress NQO1,[9] it is plausible to evaluate the cytotoxicity of the LPC/PTX combination against pancreatic cancer cells. Here, we investigated the cytotoxicity of LPC/PTX combination against four different human pancreatic cancer cells with high overexpression of NQO1[50] (i.e., PANC-1, MIA PaCa-2, Capan-1, and BXPC-3).

Interestingly, we observed that PTX is not an ideal monotherapy against these pancreatic cancer cells. In none of these four cell lines could PTX achieve a complete cancer elimination even after >10 μM of PTX was introduced into the cell culture. Followed by a sharp initial cell death upon the addition of PTX, ~40%, 50−60%, and ~80% cells remained alive in the PANC-1 or MIA PaCa-2 cells, the Capan-1 cell, and the PXPC-3 cells, respectively. As reported, PTX is often not sensitive enough to kill pancreatic cancer cells because AURKA/STK15/BTAK gene that is involved in the regulation of centrosomes and segregation of chromosomes is often amplified and overexpressed in pancreatic cancer. This could have diminished the cytotoxicity of PTX that impairs the G_2/M transition.[51] In contrast, although LPC is not as cytotoxic as PTX toward these cells at low drug concentration (<3 μM), with the increase of LPC concentration, the cytotoxic effect of LPC continued until complete cell death was achieved in all of these four pancreatic cancer cell lines. Furthermore, the combination of LPC and PTX (1L1P) showed significantly lower IC_{50} values than either single agents, when used against PANC-1, MIA PaCa-2, and Capan-1 (Figure 10, Table 4). The IC_{50} values of the LPC/PTX micelles were 0.02, 0.03, and 0.45 μM, respectively, compared with 0.81, 1.25, and 2.23 μM of LPC as a single agent, and 0.19, 0.07, and 4.91 μM of PTX as a single agent (Table 4). The CI analysis also indicated strong LPC/PTX cytotoxic synergy as the CI values are all much less than 1 in these three cell lines. For BXPC-3 cells, 1L1P showed similar cytotoxicity as the pure LPC, and there was no significantly measurable synergy with PTX. This is not surprising since PTX by itself has very minimal effect against BXPC-3 cells.

4. CONCLUSION

Through the molecular interactions between LPC and PTX, we successfully coencapsulated LPC, an extremely fast crystallizing anticancer agent, with PTX into the PEG−PLA micelles with significantly (>10 times) improved drug encapsulation efficiency and drug concentration in the micelle formulation. This approach has the potential to overcome the drug delivery challenge to intravenously deliver a poorly soluble, yet fast crystallizing drug with a stable and practically viable formulation. This design does not require toxic excipients, organic solvents, or tailor-synthesized new polymeric excipients,[23,52,53] which would certainly generate hurdles along the potential future clinical translation.

Encapsulation of more than one drugs within the polymeric micelles was previously reported to show potentials in overcoming drug resistance and improve anticancer efficacy.[54,55] In this work, the LPC/PTX combination micelles demonstrated a unique and strong pharmacological synergy against multiple NQO1-overexpressing NSCLC and pancreatic cancer cells. It is also worth noting that PTX has already been used against NSCLC and pancreatic cancers in clinic.[56−58] The combination with LPC, a NQO1-dependent anticancer agent, could bring a novel pharmacological mechanism into the current PTX therapy. With the successful development of LPC/PTX combination micelles, we are now ready to evaluate their safety and antitumor efficacy against NSCLC and pancreatic cancers. The *in vivo* evaluation of the combination micelles in several NSCLC and pancreatic tumor models is currently ongoing in our lab, and the results will be reported in the near future.

DOI: 10.1021/acs.molpharmaceut.5b00448
Mol. Pharmaceutics XXXX, XXX, XXX−XXX

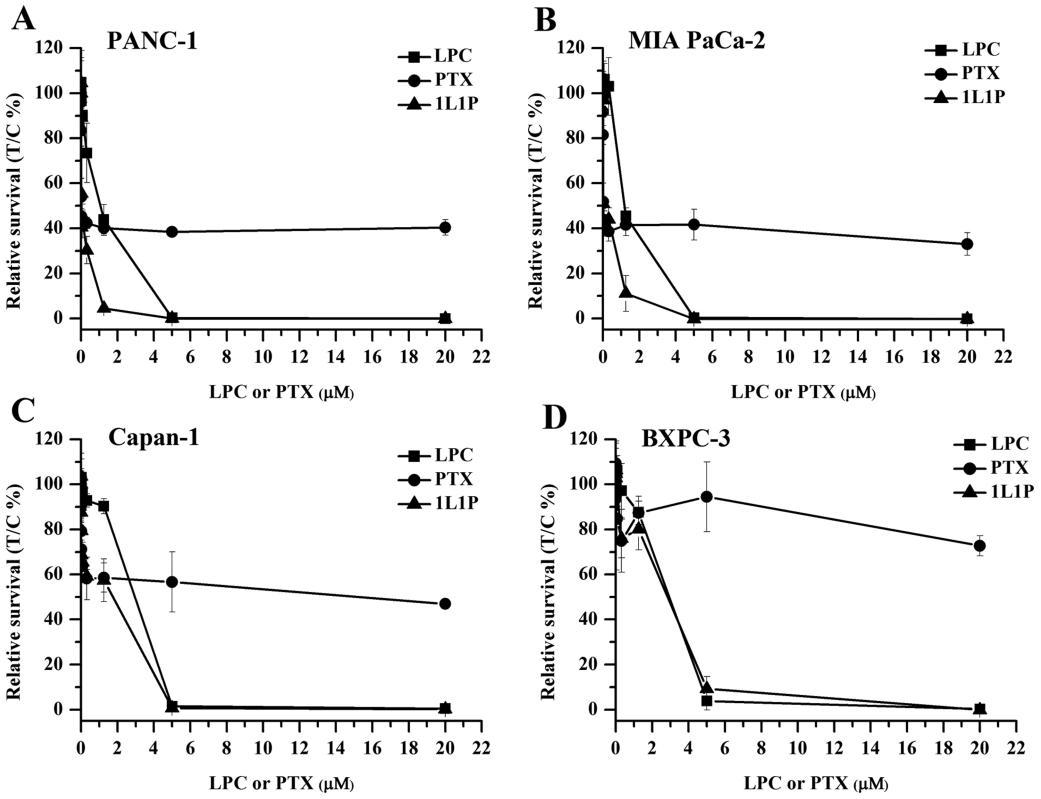

Figure 10. Cytotoxicity of LPC, PTX, and the LPC/PTX combination (1:1 molar ratio, 1L1P) against four pancreatic cancer cells: (A) PANC-1, (B) MIA PaCa-2, (C) Capan-1, and (D) BXPC-3 with the CellTiter-GloReagent assay.

Table 4. IC_{50} Values of LPC, PTX, and the LPC/PTX Combination at 1:1 Molar Ratio (1L1P) against Four Different Pancreatic Cancer Cells after 48 h of Drug Incubation. Calculated IC_{50} of the LPC/PTX Combination at 1:1 Molar Ratio (1L1P) Was Based on the Single Drug Concentration. Refer to Section 2.4.5 for the Definition and Calculation of CI and Fa Values

	IC_{50} (μM)			
drug	PANC-1	MIA PaCa-2	Capan-1	BXPC-3
LPC	0.81	1.25	2.28	2.00
PTX	0.19	0.07	4.91	>10 000
1L1P	0.02	0.03	0.45	1.86
CI (F_a = 0.5)	0.14	0.35	0.07	0.79

■ ASSOCIATED CONTENT

Supporting Information

The Supporting Information is available free of charge on the ACS Publications website at DOI: 10.1021/acs.molpharmaceut.5b00448.

Change of ^{13}C NMR chemical shifts of LPC and PTX in $CDCl_3$ solution compared with pure drug solution at the same concentration; PXRD spectra of pure LPC, pure PTX, and coprecipitated LPC and PTX mixture at 3:1 molar ratio (PDF)

■ AUTHOR INFORMATION

Corresponding Author

*E-mail: qianfeng@biomed.tsinghua.edu. Phone: (+86) 010-62794733.

Notes

The authors declare no competing financial interest.

■ ACKNOWLEDGMENTS

This research is supported by Beijing Municipal Science and Technology Commission. F.Q. also acknowledges the start-up funds provided by the Center for Life Sciences at Tsinghua and Peking Universities (Beijing, China), and by the China Recruitment Program of Global Experts. The authors thank Prof. Meixiang Wang (Department of Chemistry) and Prof. Yefeng Tang (Department of Pharmacology and Pharmaceutical Sciences) at Tsinghua University for helpful discussions regarding the characterization of physical interactions between drugs.

■ REFERENCES

(1) Gomez Castellanos, J. R.; Prieto, J. M.; Heinrich, M. Red Lapacho (Tabebuia impetiginosa)–a global ethnopharmacological commodity? *J. Ethnopharmacol.* **2009**, *121* (1), 1−13.

(2) Pink, J. J.; Planchon, S. M.; Tagliarino, C.; et al. NAD(P)H:Quinone oxidoreductase activity is the principal determinant of beta-lapachone cytotoxicity. *J. Biol. Chem.* **2000**, *275* (8), 5416−24.

(3) De Almeida, E. R. Preclinical and clinical studies of lapachol and beta-lapachone. *Open Nat. Prod. J.* **2009**, *2*, 42−47.

(4) Bentle, M. S.; Bey, E. A.; Dong, Y.; et al. New tricks for old drugs: the anticarcinogenic potential of DNA repair inhibitors. *J. Mol. Histol.* **2006**, *37* (5−7), 203−18.

(5) Dinkova-Kostova, A. T.; Talalay, P. NAD(P)H:quinone acceptor oxidoreductase 1 (NQO1), a multifunctional antioxidant enzyme and exceptionally versatile cytoprotector. *Arch. Biochem. Biophys.* **2010**, *501* (1), 116−23.

(6) Nioi, P.; Hayes, J. D. Contribution of NAD(P)H:quinone oxidoreductase 1 to protection against carcinogenesis, and regulation of its gene by the Nrf2 basic-region leucine zipper and the

DOI: 10.1021/acs.molpharmaceut.5b00448
Mol. Pharmaceutics XXXX, XXX, XXX−XXX

arylhydrocarbon receptor basic helix-loop-helix transcription factors. *Mutat. Res., Fundam. Mol. Mech. Mutagen.* **2004**, *555* (1−2), 149−71.
(7) Bey, E. A.; Bentle, M. S.; Reinicke, K. E.; et al. An NQO1- and PARP-1-mediated cell death pathway induced in non-small-cell lung cancer cells by beta-lapachone. *Proc. Natl. Acad. Sci. U. S. A.* **2007**, *104* (28), 11832−7.
(8) Belinsky, M.; Jaiswal, A. K. NAD(P)H:quinone oxidoreductase1 (DT-diaphorase) expression in normal and tumor tissues. *Cancer Metastasis Rev.* **1993**, *12* (2), 103−17.
(9) Jaiswal, A. K. Regulation of genes encoding NAD(P)H:quinone oxidoreductases. *Free Radical Biol. Med.* **2000**, *29* (3−4), 254−62.
(10) Reinicke, K. E.; Bey, E. A.; Bentle, M. S.; et al. Development of beta-lapachone prodrugs for therapy against human cancer cells with elevated NAD(P)H:quinone oxidoreductase 1 levels. *Clin. Cancer Res.* **2005**, *11* (8), 3055−64.
(11) Lien, Y. C.; Kung, H. N.; Lu, K. S.; et al. Involvement of endoplasmic reticulum stress and activation of MAP kinases in beta-lapachone-induced human prostate cancer cell apoptosis. *Histol. Histopathol.* **2008**, *23* (11), 1299−308.
(12) Ough, M.; Lewis, A.; Bey, E. A.; et al. Efficacy of beta-lapachone in pancreatic cancer treatment: exploiting the novel, therapeutic target NQO1. *Cancer Biol. Ther.* **2005**, *4* (1), 102−9.
(13) Lewis, A. M.; Ough, M.; Hinkhouse, M. M.; et al. Targeting NAD(P)H:quinone oxidoreductase (NQO1) in pancreatic cancer. *Mol. Carcinog.* **2005**, *43* (4), 215−24.
(14) Awadallah, N. S.; Dehn, D.; Shah, R. J.; et al. NQO1 expression in pancreatic cancer and its potential use as a biomarker. *Appl. Immunohistochem. Mol. Morphol.* **2008**, *16* (1), 24−31.
(15) Nasongkla, N.; Wiedmann, A. F.; Bruening, A.; et al. Enhancement of solubility and bioavailability of beta-lapachone using cyclodextrin inclusion complexes. *Pharm. Res.* **2003**, *20* (10), 1626−33.
(16) Blanco, E.; Bey, E. A.; Khemtong, C.; et al. Beta-lapachone micellar nanotherapeutics for non-small cell lung cancer therapy. *Cancer Res.* **2010**, *70* (10), 3896−904.
(17) Hartner, L.; Rosen, L.; Hensley, M.; et al. Phase 2 dose multicenter, open-label study of ARQ 501, a checkpoint activator, in adult patients with persistent, recurrent or metastatic leiomyosarcoma (LMS). *J. Clin Oncol* **2007**, *25*, 20521.
(18) Kawecki, A.; Adkins, D.; Cunningham, C.; et al. A phase II study of ARQ 501 in patients with advanced squamous cell carcinoma of the head and neck. *J. Clin Oncol* **2007**, *25*, 16509.
(19) Khong, H.; Dreisbach, L.; Kindler, H.; et al. A phase 2 study of ARQ 501 in combination with gemcitabine in adult patients with treatment naive, unresectable pancreatic adenocarcinoma. *J. Clin Oncol* **2007**, *25*, 15017.
(20) Shapiro, G.; Supko, J.; Ryan, D.; et al. Phase I trial of ARQ 501, an activated checkpoint therapy (ACT) agent, in patients with advanced solid tumors. *J. Clin. Oncol* **2005**, *23*, 3042.
(21) Gaucher, G.; Marchessault, R. H.; Leroux, J. C. Polyester-based micelles and nanoparticles for the parenteral delivery of taxanes. *J. Controlled Release* **2010**, *143* (1), 2−12.
(22) Kim, T. Y.; Kim, D. W.; Chung, J. Y.; et al. Phase I and pharmacokinetic study of Genexol-PM, a cremophor-free, polymeric micelle-formulated paclitaxel, in patients with advanced malignancies. *Clin. Cancer Res.* **2004**, *10* (11), 3708−16.
(23) Cabral, H.; Kataoka, K. Progress of drug-loaded polymeric micelles into clinical studies. *J. Controlled Release* **2014**, *190*, 465−76.
(24) He, C.; Hu, Y.; Yin, L.; et al. Effects of particle size and surface charge on cellular uptake and biodistribution of polymeric nanoparticles. *Biomaterials* **2010**, *31* (13), 3657−66.
(25) Zheng, N.; Dai, W.; Du, W.; et al. A novel lanreotide-encoded micelle system targets paclitaxel to the tumors with overexpression of somatostatin receptors. *Mol. Pharmaceutics* **2012**, *9* (5), 1175−88.
(26) Blanco, E.; Bey, E. A.; Dong, Y.; et al. Beta-lapachone-containing PEG-PLA polymer micelles as novel nanotherapeutics against NQO1-overexpressing tumor cells. *J. Controlled Release* **2007**, *122* (3), 365−74.
(27) Singla, A. K.; Garg, A.; Aggarwal, D. Paclitaxel and its formulations. *Int. J. Pharm.* **2002**, *235* (1), 179−192.
(28) Bonomi, P.; Kim, K.; Fairclough, D.; et al. Comparison of survival and quality of life in advanced non-small-cell lung cancer patients treated with two dose levels of paclitaxel combined with cisplatin versus etoposide with cisplatin: results of an Eastern Cooperative Oncology Group trial. *J. Clin Oncol* **2000**, *18* (3), 623−31.
(29) Kelly, K.; Crowley, J.; Bunn, P. A., Jr.; et al. Randomized phase III trial of paclitaxel plus carboplatin versus vinorelbine plus cisplatin in the treatment of patients with advanced non-small-cell lung cancer: a Southwest Oncology Group trial. *J. Clin Oncol* **2001**, *19* (13), 3210−8.
(30) D'Anneo, A.; Augello, G.; Santulli, A.; et al. Paclitaxel and beta-lapachone synergistically induce apoptosis in human retinoblastoma Y79 cells by downregulating the levels of phospho-Akt. *J. Cell. Physiol.* **2010**, *222* (2), 433−43.
(31) Li, C. J.; Li, Y. Z.; Pinto, A. V.; et al. Potent inhibition of tumor survival in vivo by beta-lapachone plus taxol: combining drugs imposes different artificial checkpoints. *Proc. Natl. Acad. Sci. U. S. A.* **1999**, *96* (23), 13369−74.
(32) Planchon, S. M.; Wuerzberger, S.; Frydman, B.; et al. Beta-lapachone-mediated apoptosis in human promyelocytic leukemia (HL-60) and human prostate cancer cells: a p53-independent response. *Cancer Res.* **1995**, *55* (17), 3706−11.
(33) Tao, J.; Sun, Y.; Zhang, G. G.; et al. Solubility of small-molecule crystals in polymers: D-mannitol in PVP, indomethacin in PVP/VA, and nifedipine in PVP/VA. *Pharm. Res.* **2009**, *26* (4), 855−64.
(34) Cho, Y. W.; Lee, J.; Lee, S. C.; et al. Hydrotropic agents for study of in vitro paclitaxel release from polymeric micelles. *J. Controlled Release* **2004**, *97* (2), 249−57.
(35) Labarca, C.; Paigen, K. A simple, rapid, and sensitive DNA assay procedure. *Anal. Biochem.* **1980**, *102* (2), 344−52.
(36) Chou, T. C.; Talalay, P. Quantitative analysis of dose-effect relationships: the combined effects of multiple drugs or enzyme inhibitors. *Adv. Enzyme Regul.* **1984**, *22*, 27−55.
(37) Cunha-Filho, M. S.; Landin, M.; Martinez-Pacheco, R.; et al. Beta-lapachone. *Acta Crystallogr., Sect. C: Cryst. Struct. Commun.* **2006**, *62* (8), o473−5.
(38) Zhu, Q.; Harris, M. T.; Taylor, L. S. Time-resolved SAXS/WAXS study of the phase behavior and microstructural evolution of drug/PEG solid dispersions. *Mol. Pharmaceutics* **2011**, *8* (3), 932−9.
(39) Nishi, T.; Wang, T. Melting point depression and kinetic effects of cooling on crystallization in poly (vinylidene fluoride)-poly (methyl methacrylate) mixtures. *Macromolecules* **1975**, *8* (6), 909−915.
(40) Hoei, Y.; Yamaura, K.; Matsuzawa, S. A lattice treatment of crystalline solvent-amorphous polymer mixtures on melting point depression. *J. Phys. Chem.* **1992**, *96* (26), 10584−10586.
(41) Sun, Y.; Tao, J.; Zhang, G. G.; et al. Solubilities of crystalline drugs in polymers: an improved analytical method and comparison of solubilities of indomethacin and nifedipine in PVP, PVP/VA, and PVAc. *J. Pharm. Sci.* **2010**, *99* (9), 4023−31.
(42) Chen, Y.; Liu, C.; Chen, Z.; et al. Drug-polymer-water interaction and its implication for the dissolution performance of amorphous solid dispersions. *Mol. Pharmaceutics* **2015**, *12* (2), 576−89.
(43) Matsumura, Y.; Maeda, H. A new concept for macromolecular therapeutics in cancer chemotherapy: mechanism of tumoritropic accumulation of proteins and the antitumor agent smancs. *Cancer Res.* **1986**, *46* (12 Pt 1), 6387−92.
(44) Vasey, P. A.; Kaye, S. B.; Morrison, R.; et al. Phase I clinical and pharmacokinetic study of PK1 [N-(2-hydroxypropyl)methacrylamide copolymer doxorubicin]: first member of a new class of chemotherapeutic agents-drug-polymer conjugates. Cancer Research Campaign Phase I/II Committee. *Clin. Cancer Res.* **1999**, *5* (1), 83−94.
(45) Liboiron, B. D.; Mayer, L. D. Nanoscale particulate systems for multidrug delivery: towards improved combination chemotherapy. *Ther. Delivery* **2014**, *5* (2), 149−71.
(46) Morton, S. W.; Lee, M. J.; Deng, Z. J.; et al. A nanoparticle-based combination chemotherapy delivery system for enhanced tumor

DOI: 10.1021/acs.molpharmaceut.5b00448
Mol. Pharmaceutics XXXX, XXX, XXX−XXX

killing by dynamic rewiring of signaling pathways. *Sci. Signaling* **2014**, *7* (325), ra44.
(47) Rahib, L.; Smith, B. D.; Aizenberg, R.; et al. Projecting cancer incidence and deaths to 2030: the unexpected burden of thyroid, liver, and pancreas cancers in the United States. *Cancer Res.* **2014**, *74* (11), 2913−21.
(48) Hidalgo, M. Pancreatic cancer. *N. Engl. J. Med.* **2010**, *362* (17), 1605−17.
(49) Erkan, M.; Hausmann, S.; Michalski, C. W.; et al. The role of stroma in pancreatic cancer: diagnostic and therapeutic implications. *Nat. Rev. Gastroenterol. Hepatol.* **2012**, *9* (8), 454−67.
(50) Li, L. S.; Bey, E. A.; Dong, Y.; et al. Modulating endogenous NQO1 levels identifies key regulatory mechanisms of action of beta-lapachone for pancreatic cancer therapy. *Clin. Cancer Res.* **2011**, *17* (2), 275−85.
(51) Hata, T.; Furukawa, T.; Sunamura, M.; et al. RNA interference targeting aurora kinase a suppresses tumor growth and enhances the taxane chemosensitivity in human pancreatic cancer cells. *Cancer Res.* **2005**, *65* (7), 2899−905.
(52) Murakami, M.; Cabral, H.; Matsumoto, Y.; et al. Improving drug potency and efficacy by nanocarrier-mediated subcellular targeting. *Sci. Transl. Med.* **2011**, *3* (64), 64ra2.
(53) Gao, X.; Huang, Y.; Makhov, A. M.; et al. Nanoassembly of surfactants with interfacial drug-interactive motifs as tailor-designed drug carriers. *Mol. Pharmaceutics* **2013**, *10* (1), 187−98.
(54) Shin, H. C.; Alani, A. W.; Rao, D. A.; et al. Multi-drug loaded polymeric micelles for simultaneous delivery of poorly soluble anticancer drugs. *J. Controlled Release* **2009**, *140* (3), 294−300.
(55) Shin, H. C.; Alani, A. W.; Cho, H.; et al. A 3-in-1 polymeric micelle nanocontainer for poorly water-soluble drugs. *Mol. Pharmaceutics* **2011**, *8* (4), 1257−65.
(56) Rowinsky, E. K.; Jiroutek, M.; Bonomi, P.; et al. Paclitaxel steady-state plasma concentration as a determinant of disease outcome and toxicity in lung cancer patients treated with paclitaxel and cisplatin. *Clinical cancer research: an official journal of the American Association for Cancer Research* **1999**, *5* (4), 767−74.
(57) Bonomi, P. Review of paclitaxel/carboplatin in advanced non-small cell lung cancer. *Seminars in oncology* **1999**, *26* (1 Suppl 2), 55−9.
(58) Von Hoff, D. D.; Ervin, T.; Arena, F. P.; et al. Increased survival in pancreatic cancer with nab-paclitaxel plus gemcitabine. *N. Engl. J. Med.* **2013**, *369* (18), 1691−703.

DOI: 10.1021/acs.molpharmaceut.5b00448
Mol. Pharmaceutics XXXX, XXX, XXX−XXX